Femtogram Electrochemical Sensing of Prion Proteins Using Quantum Dots

Pavlina Sobrova[1,2], *Marketa Ryvolova*[1,2], *Vladimir Pekarik*[3], *Jaromir Hubalek*[1,2], *Vojtech Adam*[1,2], *Rene Kizek*[1,2,*]

[1] Department of Chemistry and Biochemistry, Faculty of Agronomy, Mendel University in Brno, Zemedelska 1, CZ-613 00 Brno, Czech Republic, European Union
[2] Central European Institute of Technology, Brno University of Technology, Technicka 3058/10, CZ-616 00 Brno, Czech Republic, European Union
[3] Department of Cellular and Molecular Neurobiology, Central European Technology Institute, Masaryk University, Kamenice 735/3, CZ-625 00 Brno, Czech Republic, European Union
[*]E-mail: kizek@sci.muni.cz

The prion protein (PrP) is involved in neurodegeneration via its conversion from the normal cellular form, PrP^C, to the infectious form, PrP^{Sc}, which is the causative agent of the transmissible spongiform encephalopathies (TSEs) including Creutzfeldt-Jakob disease (CJD). In spite of great effort in this field, diagnostics of prion protein caused diseases represents a sort of challenge. In this study, we aimed our attention on studying of prion protein interaction with CdTe quantum dots (QDs) by voltammetry as a new and extremely sensitive tool for sensing of these proteins. Primarily, we characterized fluorescent and electrochemical properties of QDs. Further, electrochemical study of their interactions was carried out to find the most suitable conditions for sensitive detection of prion proteins. Detection limit (3 S/N) was estimated as 1 fg in 5 µl. This makes labeling of proteins with QDs of great importance due to easy applicability and possibility to use in miniaturized devices, which can be used *in situ*. Based on our results it can be concluded that QDs-prion protein complex is stable and can be quantified in extremely low amounts. This should open new possibilities how to determine the presence of these proteins on surgical equipment and other types of materials, which could be contagious.

1. INTRODUCTION

Prion protein occurs in all mammal cells, primarily in neural cells and immune system cells. Its physiological function is not completely clear, however it is assumed that participates on synaptic

transfer and cell differentiation. The prion protein (PrP) is involved in neurodegeneration via its conversion from the normal cellular form, PrP^C, to the infectious form, PrP^{Sc}, which is the causative agent of the transmissible spongiform encephalopathies (TSEs) including Creutzfeldt-Jakob disease (CJD) [1-4]. The coexistence of Alzheimer disease pathology in Creutzfeld-Jakob disease (CJD) has been reported [5]. Transfer of infectious prion proteins from animal to animal has been numerous times described [2,6,7], however, it was discovered recently prion proteins could cling to surgical equipment used on CJD patients and then infect others, because normal sterilization techniques do not kill the hardy proteins [8]. The risks of transmission are low, but it might occur if hospitals do not discard all CJD-contaminated surgical tools or strip them of prions using chemicals and ultra-high temperature. Until now, most attention has been focused on treating dirty equipment after neurosurgery, from which five patients have caught CJD [9], but the transmission might also happen from patients incubating the disease who have operations before they begin to show symptoms.

Diagnostics of prion protein caused diseases represents a sort of challenge [10,11]. In the case of human diseases, diagnosis is based almost exclusively on clinical examination and the disease is then considered as probable depending on the extent to which the clinical symptoms fit the standard guidelines. Currently, PrP^{Sc} is the only disease-specific analyte commercially used for identification of prion diseases [12]. From the clinical point of view, the most sensitive and specific method of diagnosing TSE is unquestionably experimental infection in laboratory animals. The animal is injected with a homogenate prepared from the suspicious tissue and appearance of clinical signs is followed. The disease development is then confirmed after dissection using classic techniques (histology, immunohistology, Western Blot). These methods are too laborious and time-consuming to be used for routine high-throughput screening [13]. Recently, new post-mortem tests have been introduced enabling rapid screening of the suspicious samples. Currently five commercial tests are approved by the European Commission for BSE detection (Prionics-Check Western test, Enfer test, CEA/Biorad test, Prionics-Check LIA test, and Conformational-dependent immunoassay). All these tests are based on immunodetection of the pathological PrP^{Sc} isoform; four of them use proteolysis to distinguish PrP^C from misfolded PrP^{Sc} [10]. It has to be noted that none of these tests is able to identify infected animal at the pre-symptomatic stage. A possibility how to diagnose prion protein related neurodegenerative disease is to use Protein-misfolding cyclic amplification (PMCA) [14]. Method is based on converting additional normal prion protein to the sample with infectious prion. PMCA involves repeated cycles on incubation and sonication. These repeated cycles can amplify the amount of prion protein present in the sample from four to 40 times in two weeks [15,16]. Sensitive and specific detection of abnormal prion protein in blood could provide a diagnostic test or screening assay for animal and human prion diseases. Therefore, diagnostic tests of prion diseases present a unique challenge requiring development of novel assays exploiting properties uniquely possessed by this misfolded protein complex.

The characterization and analysis of biomolecules and biological systems in the context of intact organisms is known as *in vivo* research. A new and exciting direction of research for quantum dots (QDs) is their application as a contrast agent for *in vivo* imaging [17-28]. For most investigations of *in vivo* imaging, QDs are usually directly injected into the live animal intravenously or subcutaneously and thereby are delivered into the bloodstream. The behavior of QDs *in vivo* is very

interesting because they have to interact with the components of plasma, blood cells, and the vascular endothelium. QDs are mainly applied for imaging of cancer cells [29-31], however, prion proteins have not been sensed by these particles yet. Therefore, we aimed our attention on studying of prion protein interaction with CdTe QDs by voltammetry as a new and extremely sensitive tool for sensing of these proteins.

2. EXPERIMENTAL PART

2.1 Chemicals and material

Cadmium chloride, sodium tellurite, mercaptopropionic acid and other used chemicals were purchased from Sigma Aldrich (St. Louis, USA). Stock solutions of 50 µg mL^{-1} of Cd^{2+}, and 500 µg/ml of MPA were prepared daily and subsequently diluted to the appropriate concentration. Acetate buffer of pH 5 was prepared with 0.2 M acetic acid and 0.2 M sodium acetate, diluted with ACS water and used as a supporting electrolyte. Prion - Recombinant bovine PrP (highly purified protein (rec bovPrP), amino acid sequence corresponding to mature bovine PrP (amino acids 25 - 242), Expressed in an *E. coli* K12 strain, MW 23 686 Da) was purchased from Prionics AG (Switzerland). High purity deionized water (Milli-Q Millipore 18.2 MΩ cm^{-1}, Bedford, MA, USA) was used throughout the study.

2.2 Microwave assisted preparation of quantum dots

QD were prepared according to Duan et al. [32]. Cadmium chloride solution (CdCl$_2$, 0.04 M, 4 mL) was diluted to 42 mL with ultrapure water, and then trisodium citrate dihydrate (100 mg), Na$_2$TeO$_3$ (0.01 M, 4 mL), MPA (119 mg), and NaBH$_4$ (50 mg) were added successively under magnetic stirring. The molar ratio of Cd^{2+}/MPA/Te was 1:7:0.25. 10 mL of the resulting CdTe precursor was put into a Teflon vessel. CdTe QDs were prepared at 95°C for various times according to desired color (10 min. – green, 30 min. yellow, 120 min. – red) under microwave irradiation (400 W, Multiwave3000, Anton-Paar GmbH, Austria). After microwave irradiation, the mixture was cooled 50 °C and the CdTe QDs sample was obtained. Repurification of CdTe QDs was carried out using isopropanol condensing. The CdTe QDs was mixed with isopropanol in ratio 1:2 and then centrifuged 10 minutes under 25000 rpm (Eppendorf centrifuge 5417R). Supernatant (clear CdTe QDs) was than resuspended in initial volume of Tris Buffer pH 8.5.

2.3 Transmission electron microscope

Morphology studies and phase analysis were carried out with the transmission electron microscope (TEM) Philips CM 12 (tungsten cathode, using a 120kV electron beam). Chemical compositions were studied by energy-dispersive X – ray spectroscopy (EDX). Electron diffraction patterns were simulated by JEMS software. Samples for TEM measurements were prepared by placing

drops of the solution (sample and water) on coated Cu grids (holey carbon and holey SiO_2/SiO) and subsequently drying in air.

2.4 Spectroscopy

Absorbance and fluorescence spectra were acquired by multifunctional microplate reader Tecan Infinite 200 PRO (TECAN, Switzerland). The sample (50 μL) was placed in a transparent 96 well microplate with flat bottom (Nunc, Thermo Scientific, Germany). Absorbance scan was measured in the range from 230 – 1000 nm using 5 nm steps. 350 nm was used as an excitation wavelength and the fluorescence scan within the range from 400 to 850 nm (5 nm steps). The detector gain was set to 50. For both absorbance and fluorescence measurements, each value was an average of 5 measurements.

2.5 Electrochemical analyzer

Electrochemical measurements were performed with AUTOLAB Analyzer (EcoChemie, Netherlands) connected to VA-Stand 663 (Metrohm, Switzerland), using a standard cell with three electrodes. The working electrode was a hanging mercury drop electrode (HMDE) with a drop area of 0.4 mm^2. The reference electrode was an Ag/AgCl/3M KCl electrode and the auxiliary electrode was a graphite electrode. Acetate buffer (0.2 M, pH 5) was used as the supporting electrolyte. For smoothing and baseline correction the software GPES 4.9 supplied by EcoChemie was employed. The amount of QDs was measured using DPV. Differential pulse voltammetric measurements were carried out under the following parameters: start potential -1.5 V; end potential 0 V; a modulation time 0.057 s, a time interval 0.2 s, a step potential of 1.05 mV s^{-1}, a modulation amplitude of 250 mV, E_{ads} = 0 V. All experiments were carried out at room temperature (20 °C). The DPV samples analyzed were deoxygenated prior to measurements by purging with argon (99.999%) saturated with water for 120 s.

2.6 Descriptive statistics and estimation of detection limit

Data were processed using MICROSOFT EXCEL® (USA). Results are expressed as mean ± standard deviation (S.D.) unless noted otherwise (EXCEL®). The detection limits (LOD, 3 signal/noise, S/N) were calculated according to Long and Winefordner [33], whereas N was expressed as standard deviation of noise determined in the signal domain unless stated otherwise.

3. RESULTS AND DISCUSSION

3.1 TEM characterization of synthesized quantum dots

The TEM examination of prepared CdTe QDs indicated the morphology and phase composition were clearly homogeneous. The TEM pictures (at higher magnifications) showed that dried droplets consists of a fine grain powder of a typical size of particles below 10 nm (Fig. 1A).

Chemical and phase compositions were proved by EDAX measurements and by electron diffraction (SEAD), respectively (bottom inset in Fig. 1A). A width of the diffraction rings corresponding to the observed small particles size. Other morphological structures were not found and other phases were not distinguished on both type TEM grid (carbon and silicon oxide). When we found that we synthesized objects smaller than 10 nm, we followed with their optical characterization. QDs solution under UV light illumination is shown in upper inset in Fig. 1A. Optical properties of synthesized QDs were characterized spectrometrically. From the absorbance spectra it follows that QDs absorb strongly the light in the UV range, however also the absorption maximum at 500 nm was observed. From the emission spectrum shown in Fig. 1B it is apparent that CdTe QDs are exhibiting strong fluorescence with the emission maximum at 525 nm. It can be concluded based on the results obtained that we successfully synthesized CdTe QDs. In the following parts of our experiments, we aimed our attention at their electrochemical characterization.
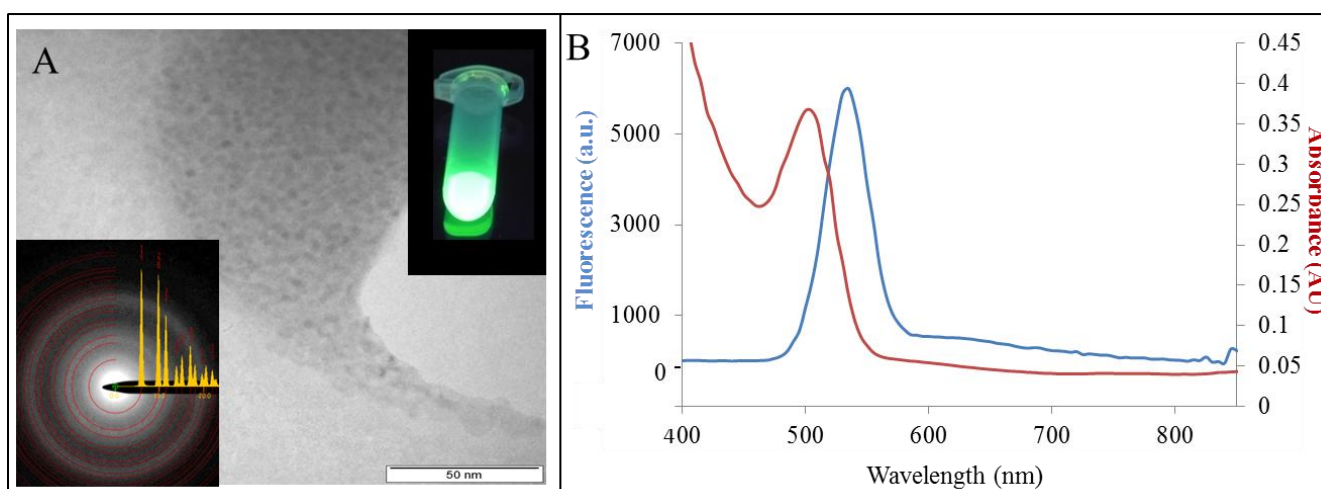

Figure 1. (**A**) TEM micrograph of the sample showing fine morphologies of QDs with the typical particles size below 10 nm; in inset: QDs solution under UV light illumination. (**B**) Absorption and emission spectra of CdTe QDs.

3.2 Sensing of prion proteins

Due to the presence of MPA on the surface of QDs, good interaction with proteins can be expected. Sensing of proteins is of extreme interest for numerous scientists. In this study, we studied prion proteins, which are biomolecules naturally occurring in the animal cells. 3D model of prion protein structure is shown in inset in Fig. 2A. We mixed prion protein (500 µg mL^{-1}) with QDs (500 µg mL^{-1}) in ratios 1:1, 1:2, 1:3, 1:4, 1:5, 1:6, 1:7, 1:7, 1:8, 1:9 and 1:10, and vice versa, and let to interact at 35 °C in dark for 24 hours. This mixture was the analyzed by adsorptive transfer stripping technique (AdTS) coupled with differential pulse voltammetry. The main principle is based in electrode removing from a solution after accumulating of a target molecule on its surface, rinsing of the electrode and transferring to a pure supporting electrolyte, where no interferences are present. The scheme of adsorptive transfer stripping technique (AdTS) can be summarized to the following steps:

(1) renewing of a surface of a working electrode; (2) adsorbing of target molecule in a drop solution onto the surface at open circuit and/or superimposed potential; (3) washing the working electrode in a solution; (4) transferring of the washed electrode to a supporting electrolyte; (5) measurement of adsorbed target molecules. Using AdTS DPV we found that QDs itself did not adsorb on the surface of working electrode (not shown).
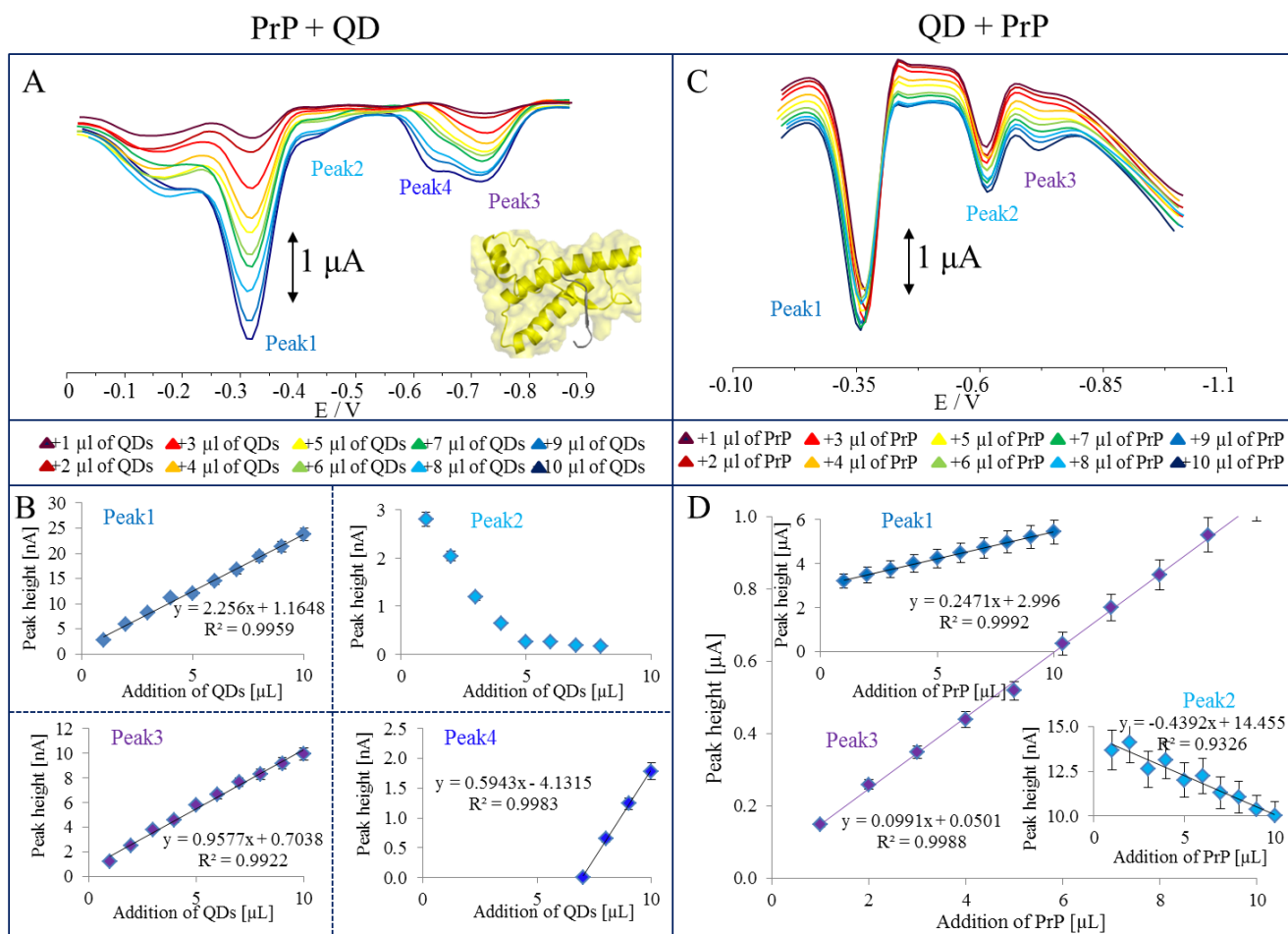

Figure 2. (**A**) DP voltammograms of prion protein (PrP, 500 μg mL^{-1}) with additions of QDs in various volumes (460 μg mL^{-1}, quantified according to concentration of cadmium(II)). (**B**) Dependences of peaks 1, 2, 3 and 4 heights on the concentration of QDs. (**C**) DP voltammograms of QDs (460 μg mL^{-1}) with additions of prion protein (PrP, 500 μg mL^{-1}) in various volumes (500 μg mL^{-1}). (**D**) Dependences of peaks 1, 2 and 3 heights on the concentration of PrP.

Therefore, QDs-prion protein complex only was adsorbed on the surface of working electrode (120 s) and measured using DPV. The increasing concentration of QDs gave us four peaks (Fig. 2A). Peak 3 corresponded to prion protein itself. It is obvious that this signal is lower compared to others. Peaks 1, 3 and 4 belong to QDs-prion protein complex. Peak 1 can be associated to Cd(II)-prion protein because of shifting of Cd(II) peak to more positive potentials due to Cd(II) interactions with protein moieties. Peaks 3 and 4 can be associated with MPA-Cd(II)-protein complexes. These

complexes can be formed by interactions of some amino acids moieties with Cd(II). Moreover, we found that peaks 1, 2 and 3 were linearly proportional to concentration of QDs, which is important for sensing of prions (Fig. 2B).
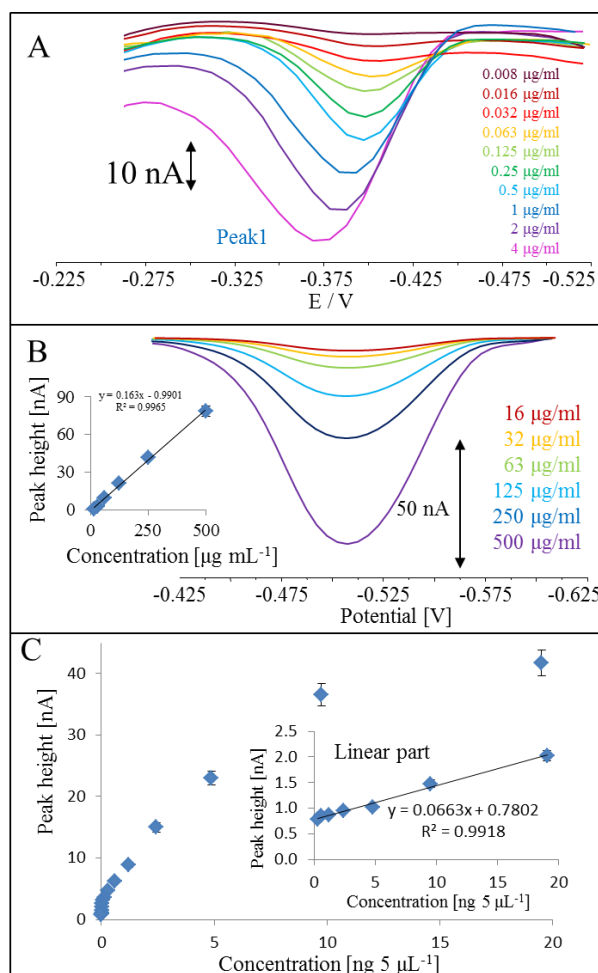

Figure 3. (**A**) 3D structure of human prion protein, expasy.org. (**B**) DP voltammograms of QDs-prion protein complex, concentration of the prion protein was as stated in the figure. The complex was measured using AdTS DPV. (**C**) DP voltammograms of various prion protein concentrations. The peak height enhanced with the increasing concentration of prion proteins. Tested concentration range was from 16 μg mL^{-1} to 500 μg mL^{-1}. The complex was measured using AdTS DPV; in inset: calibration curve with regression coefficient R^2 = 0.9972. (**D**) Calibration curves for QDs-prion protein complex.

To find the most appropriate peak, complexes of QDs with the increasing prion protein concentration were analyzed using AdTS DPV. Peak 4 disappeared, but the peaks 1, 3 and 4 remained (Fig. 2C). Peak 1 and 3 increased linearly with the increasing concentration of prions, which can be associated with the fact that nature of this peak is somewhat dependent on prion protein concentration (Fig. 2D). Peak 2 decreased with the increasing concentration of prions. The interaction of prion proteins with CdTe QDs was also confirmed by decreasing fluorescence of the particles with the increasing concentration of QDs.

It clearly follows from the results obtained that peak 1 is the most sensitive and proportional to concentration of both QDs-prion protein complex. Therefore, we aimed our attention to find detection limit of our sensing assay. The prion protein was analyzed labeled with QDs (Fig. 3A) and without labeling (Fig. 3B) both using AdTS DPV. Sensitivity of QDS labeling is of several magnitude higher compared to non-labeled prion proteins detection. The detection limit as 16 µg of prion protein per ml was estimated (3 S/N). Compared to this, we also measured calibration dependence of QDs-prion protein complex (Fig. 3C). The calibration range was from $1 \cdot 10^{-5}$ to 4 µg mL^{-1} (75 fg 5 µL^{-1} to 20 ng µL^{-1}). The obtained dependence was logarithmic, which can be related to scavenging of electrochemical peak due to the presence of excess electroactive substances. Strictly linear part was found within the interval from 0.05 ng mL^{-1} to 4 ng mL^{-1}. Detection limit (3 S/N) was estimated as 1 fg in 5 µl. This makes labeling of proteins with QDs of great importance due to easy applicability and possibility to use in miniaturized devices.

4. CONCLUSIONS

QDs, tiny light-emitting nanocrystals, have emerged as a new promising class of fluorescent probes for biomolecular and cellular imaging. In comparison with organic dyes and fluorescent proteins, QDs have unique optical and electronic properties such as size-tunable light emission, improved signal brightness, resistance against photobleaching, and simultaneous excitation of multiple fluorescence colors [34]. In this study, we found that QDs are also excellent electroactive labels for detection of prion proteins. QDs-prion protein complex is stable and can be quantified in extremely low amounts. There have been published several papers how to sense the complex of prion proteins using quantum dots [35-38], and there is also numerous papers on the electrochemistry of quantum dots and their interactions with various biomolecules [39-45], however, complex between CdTe QDs and prion proteins have never been analyzed. We showed that these complex was stable enough to by analysed both voltammetry and spectrometry, which open new possibilities how to determine the presence of these proteins on surgical equipment and other types of materials, which could be contagious. This assumption is supported also by detection limit, which belongs to ultrasensitive ones. The specificity of determination can be enhanced using specific antibodies.

References

1. M. Imran and S. Mahmood, *Virol. J.*, 8 (2011) 1.
2. S. B. Prusiner, *Proc. Natl. Acad. Sci. U. S. A.*, 95 (1998) 13363.

3. K. M. Pan, M. Baldwin, J. Nguyen, M. Gasset, A. Serban, D. Groth, I. Mehlhorn, Z. W. Huang, R. J. Fletterick, F. E. Cohen and S. B. Prusiner, *Proc. Natl. Acad. Sci. U. S. A.*, 90 (1993) 10962.
4. S. B. Prusiner, *Science*, 252 (1991) 1515.
5. J. A. Hainfellner, J. Wanschitz, K. Jellinger, P. P. Liberski, F. Gullotta and H. Budka, *Acta Neuropathol.*, 96 (1998) 116.
6. M. E. Bruce, R. G. Will, J. W. Ironside, I. McConnell, D. Drummond, A. Suttie, L. McCardle, A. Chree, J. Hope, C. Birkett, S. Cousens, H. Fraser and C. J. Bostock, *Nature*, 389 (1997) 498.
7. S. B. Prusiner, *Science*, 278 (1997) 245.
8. M. Glatzel, E. Abela, M. Maissen and A. Aguzzi, *N. Engl. J. Med.*, 349 (2003) 1812.
9. D. A. Hilton, A. C. Ghani, L. Conyers, P. Edwards, L. McCardle, D. Ritchie, M. Penney, D. Hegazy and J. W. Ironside, *J. Pathol.*, 203 (2004) 733.
10. C. Soto, *Nat. Rev. Microbiol.*, 2 (2004) 809.
11. P. Sobrova, M. Ryvolova, V. Adam and R. Kizek, *Electrophoresis*, 33 (2012) 3644.
12. A. Zsolnai, I. Anton, C. Kuhn and L. Fesus, *Electrophoresis*, 24 (2003) 634.
13. J. Grassi, S. Maillet, S. Simon and N. Morel, *Vet. Res.*, 39 (2008).
14. G. P. Saborio, B. Permanne and C. Soto, *Nature*, 411 (2001) 810.
15. C. Soto, G. P. Saborio and L. Anderes, *Trends Neurosci.*, 25 (2002) 390.
16. C. Soto, L. Anderes, S. Suardi, F. Cardone, J. Castilla, M. J. Frossard, S. Peano, P. Saa, L. Limido, M. Carbonatto, J. Ironside, J. M. Torres, M. Pocchiari and F. Tagliavini, *FEBS Lett.*, 579 (2005) 638.
17. C. Bouzigues, T. Gacoin and A. Alexandrou, *ACS Nano*, 5 (2011) 8488.
18. M. G. Lu, K. T. Al-Jamal, K. Kostarelos and J. Reineke, *ACS Nano*, 4 (2010) 6303.
19. X. H. Gao, L. L. Yang, J. A. Petros, F. F. Marshal, J. W. Simons and S. M. Nie, *Curr. Opin. Biotechnol.*, 16 (2005) 63.
20. X. Michalet, F. F. Pinaud, L. A. Bentolila, J. M. Tsay, S. Doose, J. J. Li, G. Sundaresan, A. M. Wu, S. S. Gambhir and S. Weiss, *Science*, 307 (2005) 538.
21. A. M. Smith, H. W. Duan, A. M. Mohs and S. M. Nie, *Adv. Drug Deliv. Rev.*, 60 (2008) 1226.
22. R. Hu, X. B. Zhang, R. M. Kong, X. H. Zhao, J. H. Jiang and W. H. Tan, *J. Mater. Chem.*, 21 (2011) 16323.
23. C. A. J. Lin, W. K. Chuang, Z. Y. Huang, S. T. Kang, C. Y. Chang, C. T. Chen, J. L. Li, J. K. Li, H. H. Wang, F. C. Kung, J. L. Shen, W. H. Chan, C. K. Yeh, H. I. Yeh, W. F. T. Lai and W. H. Chang, *ACS Nano*, 6 (2012) 5111.
24. Y. Zhang, G. S. Hong, Y. J. Zhang, G. C. Chen, F. Li, H. J. Dai and Q. B. Wang, *ACS Nano*, 6 (2012) 3695.
25. A. M. Dennis, W. J. Rhee, D. Sotto, S. N. Dublin and G. Bao, *ACS Nano*, 6 (2012) 2917.
26. L. Y. Guan, Y. Q. Li, S. Lin, M. Z. Zhang, J. Chen, Z. Y. Ma and Y. D. Zhao, *Anal. Chim. Acta*, 741 (2012) 86.
27. M. J. Ruedas-Rama, J. D. Walters, A. Orte and E. A. H. Hall, *Anal. Chim. Acta*, 751 (2012) 1.
28. W. J. Wang, L. Bao, J. P. Lei, W. W. Tu and H. X. Ju, *Anal. Chim. Acta*, 744 (2012) 33.
29. H. S. Mansur, *Wiley Interdiscip. Rev.-Nanomed. Nanobiotechnol.*, 2 (2010) 113.
30. A. Papagiannaros, T. Levchenko, W. Hartner, D. Mongayt and V. Torchilin, *Nanomed.- Nanotechnol. Biol. Med.*, 5 (2009) 216.
31. E. B. Voura, J. K. Jaiswal, H. Mattoussi and S. M. Simon, *Nat. Med.*, 10 (2004) 993.
32. J. L. Duan, L. X. Song and J. H. Zhan, *Nano Res.*, 2 (2009) 61.
33. G. L. Long and J. D. Winefordner, *Anal. Chem.*, 55 (1983) A712.
34. C. Frigerio, D. S. M. Ribeiro, S. S. M. Rodrigues, V. Abreu, J. A. C. Barbosa, J. A. V. Prior, K. L. Marques and J. L. M. Santos, *Anal. Chim. Acta*, 735 (2012) 9.
35. T. Tsuji, S. Kawai-Noma, C. G. Pack, H. Terajima, J. Yajima, T. Nishizaka, M. Kinjo and H. Taguchi, *Biochem. Biophys. Res. Commun.*, 405 (2011) 638.
36. J. M. Xu, P. Ruchala, Y. Ebenstain, J. J. Li and S. Weiss, *J. Phys. Chem. B*, 116 (2012) 11370.

37. L. Y. Zhang, H. Z. Zheng, Y. J. Long, C. Z. Huang, J. Y. Hao and D. B. Zhou, *Talanta*, 83 (2011) 1716.
38. Y. W. Zhou, C. M. Li, Y. Liu and C. Z. Huang, *Analyst*, 138 (2013) 873.
39. L. Krejcova, D. Dospivova, M. Ryvolova, P. Kopel, D. Hynek, S. Krizkova, J. Hubalek, V. Adam and R. Kizek, *Electrophoresis*, 33 (2012) 3195.
40. L. Krejcova, D. Huska, D. Hynek, P. Kopel, V. Adam, J. Hubalek, L. Trnkova and R. Kizek, *Int. J. Electrochem. Sci.*, 8 (2013) 689.
41. L. Krejcova, D. Hynek, V. Adam, J. Hubalek and R. Kizek, *Int. J. Electrochem. Sci.*, 7 (2012) 10779.
42. L. Krejcova, D. Hynek, P. Kopel, V. Adam, J. Hubalek, L. Trnkova and R. Kizek, *Chromatographia*, 76 (2013) 355.
43. H. Razmi and R. Mohammad-Rezaei, *Biosens. Bioelectron.*, 41 (2013) 498.
44. S. Skalickova, O. Zitka, L. Nejdl, S. Krizkova, J. Sochor, L. Janu, M. Ryvolova, D. Hynek, J. Zidkova, V. Zidek, V. Adam and R. Kizek, *Chromatographia*, 76 (2013) 345.
45. Y. F. Wu, P. Xue, Y. J. Kang and K. M. Hui, *Anal. Chem.*, 85 (2013) 3166.